Available online at www.sciencedirect.com
SCIENCE DIRECT®
PERGAMON
International Journal of Heat and Mass Transfer 46 (2003) 4467–4481
International Journal of HEAT and MASS TRANSFER
www.elsevier.com/locate/ijhmt

Heat transfer analysis of boreholes in vertical ground heat exchangers

Heyi Zeng, Nairen Diao, Zhaohong Fang *

The Ground Source Heat Pump Research Center, Shandong Institute of Architecture and Engineering, 47 Heping Road, Jinan 250014, China

Received 1 October 2002; received in revised form 25 April 2003

Abstract

A ground heat exchanger (GHE) is devised for extraction or injection of thermal energy from/into the ground. Bearing strong impact on GHE performance, the borehole thermal resistance is defined by the thermal properties of the construction materials and the arrangement of flow channels of the GHEs. Taking the fluid axial convective heat transfer and thermal "short-circuiting" among U-tube legs into account, a new quasi-three-dimensional model for vertical GHEs is established in this paper, which provides a better understanding of the heat transfer processes in the GHEs. Analytical solutions of the fluid temperature profiles along the borehole depth have been obtained. On this basis analytical expressions of the borehole resistance have been derived for different configurations of single and double U-tube boreholes. Then, different borehole configurations and flow circuit arrangements are assessed in regard to their borehole resistance. Calculations show that the double U-tubes boreholes are superior to those of the single U-tube with reduction in borehole resistance of 30–90%. And double U-tubes in parallel demonstrate better performance than those in series.

Keywords: Ground source heat pump; Ground heat exchanger; Model; Thermal resistance; Analytical solution

1. Introduction

Utilizing the ground as a heat source/sink, ground-coupled heat pump (GCHP) systems have been gaining increasing popularity for space conditioning in residential and commercial buildings due to their reduced energy and maintenance costs as compared to conventional systems. This system is environment-friendly, causing less carbon dioxide emission than their conventional alternatives. The GCHP system features its ground, or geothermal, heat exchanger (ground heat exchanger, GHE), whether it is horizontally installed in trenches or as U-tubes in vertical boreholes. The advantages of vertical GHEs are that they require smaller plots of land areas, and can yield the most efficient ground source heat pump system performance. The vertical GHEs are usually constructed by inserting one or two high-density polyethylene U-tubes in vertical boreholes to serve as the ground loops, which are referred to as single U-tube or double U-tube GHEs, respectively. The boreholes should be grouted to provide better thermal conductance and prevent groundwater from possible contamination. The single U-tube configuration has been widely used in the North American [1,2]. Being popular mainly in Europe [3], the basic construction of the double U-tube GHE consists of two U-tubes installed in one borehole and piped in either a series or parallel flow circuit. Borehole depths usually range from 40 to 200 m with diameter of 75–150 mm. A schematic diagram of a borehole with U-tubes in vertical GHEs is illustrated in Fig. 1.

* Corresponding author. Tel.: +86-531-6401003; fax: +86-531-6952404.
E-mail address: fangzh@sdai.edu.cn (Z. Fang).

0017-9310/$ - see front matter © 2003 Elsevier Ltd. All rights reserved.
doi:10.1016/S0017-9310(03)00270-9

Nomenclature

C	fluid specific heat ($J\,kg^{-1}\,K^{-1}$)
D	half spacing of U-tube shanks (m)
E, F, G	distribution functions, see Appendices A–C
H	active borehole depth (m)
k	ground thermal conductivity ($W\,m^{-1}\,K^{-1}$)
k_b	grout thermal conductivity ($W\,m^{-1}\,K^{-1}$)
M	mass flow rate of circulating fluid ($kg\,s^{-1}$)
N	number of pipes in a borehole in Eq. (1)
q	heat flow per unit length of pipe ($W\,m^{-1}$)
r_b	borehole radius (m)
r_p	pipe outer radius (m)
R	thermal resistance, defined in Eq. (4) (m K/W)
R^{Δ}	thermal resistance defined in Eq. (6) and text
R^*	dimensionless thermal resistance
R_b	effective borehole thermal resistance ($m\,K\,W^{-1}$)
R_p	thermal resistance of pipe wall ($m\,K\,W^{-1}$)
S	dimensionless thermal resistance defined in Eq. (8) and text
T_b	borehole wall temperature (°C)
T_f	fluid temperature (°C)
z	axial coordinate (m)
Z	dimensionless coordinate

Greek symbols

β	dimensionless parameter in Eq. (10)
β_0, β_1	fitted parameters in Eq. (2)
Θ	dimensionless fluid temperature

Subscripts

1, 2, 3, 4	pipe sequence in borehole
d	down-flow
u	up-flow

Superscripts

$'$	inlet temperature
$''$	outlet temperature

Despite all the advantages of the GCHP system, commercial growth of the technology has been hindered by higher capital cost of the system, of which a significant portion is attributed to GHE. In consequence, the borehole thermal resistance is critical for the economical competitiveness of GCHP systems in the heating and air-conditioning market.

It is evident that the double U-tube configuration provides more heat transfer area between the fluid and the ground than the single U-tube GHE does, and will reduce the borehole thermal resistance. On the other hand, however, it may require more pipes and consume more pumping power in operation for a certain demand. Due to complexity of the analysis few studies on comparison among the different GHE configurations have ever reported in literature so far. Thus, it remains a task for scholars and engineers to assess performances and costs of the different GHE configurations by means of analyses and practical observations.

2. Background of borehole heat transfer modeling

Heat transfer between a GHE and its surrounding soil/rock is difficult to model for the purpose of sizing the exchanger or energy analysis of the system. Besides the structural and geometrical configuration of the exchanger a lot of factors influence the exchanger performance, such as the ground temperature distribution, soil moisture content and its

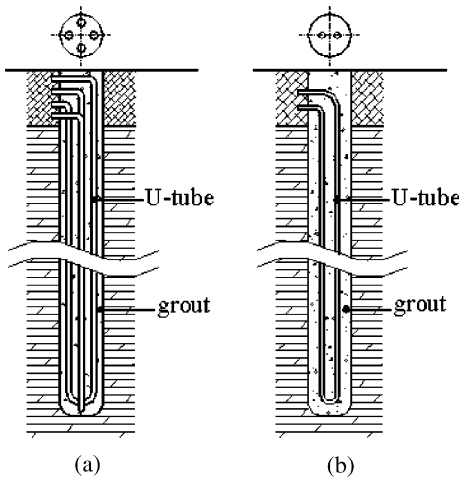

Fig. 1. Schematic diagram of boreholes in the vertical GHE: (a) double U-tube and (b) single U-tube.

thermal properties, groundwater movement and possible freezing and thawing in soil. Thus, it is crucial to work out appropriate and validated tools, by which the thermal behavior of GCHP systems can be assessed and then, optimized in technical and economical aspects.

In the GHEs the heat carrier fluid flows along the borehole in one channel down to the bottom of the borehole and back upward in another channel. In cooling mode, for instance, the warm fluid induces conductive heat flow in the surrounding cooler soil. The borehole may be conceived as a hot rod, from which heat flows to the surrounding ground. A fundamental task for application of the GCHP technology is to grasp the heat conduction process of a single borehole in the GHE. Heat transfer in a field with multiple boreholes may be analyzed on this basis by means of the superimposition principle. The design goal is to control the temperature rise of the ground and the circulating fluid within acceptable limits over the life of the system.

Involving a time span of months or even years, the heat transfer process in the GHE is rather complicated, and should be treated, on the whole, as a transient one. Because of all the complications of this problem and its long time scale, the heat transfer process may usually be analyzed in two separated regions. One is the solid soil/rock outside the borehole, where the heat conduction has to be treated as a transient process. Since the borehole depth is much larger than its diameter, this process is often formulated by the one-dimensional line-source or cylindrical-source theory [4]. A two-dimensional model of the finite line-source [5] has also been presented by the authors to consider the axial heat flow in the ground for longer durations. Variation in load and on-off cycling of the GHE can be considered by superimposition of a series of heating pulses [6]. The temperature on the borehole wall can then be determined for any instant on specified operational conditions.

Another sector isolated for analysis is the region inside the borehole, including the backfilling, the U-tubes and the circulating fluid inside the pipes. The main objective of this analysis is to determine the entering and leaving temperatures of the circulating fluid in the exchanger according to the borehole wall temperature and its heat flow. Compared with the infinite ground outside it, both the dimensional scale and thermal mass of the borehole are much smaller. Moreover, the temperature variation inside the borehole is usually slow and minor. Thus, it is a common practice that the heat transfer in this region is approximated as a steady-state process. Such simplification has been proved appropriate and convenient for most engineering practices except for analysis dealing with dynamic responses within a few hours [7]. The borehole thermal resistance is determined by a number of parameters, including the composition and flow rate of the circulating fluid, borehole diameter, grout and U-tube material as well as arrangement of flow channels.

A few models of varying complexity have been established to describe the heat transfer in the GHE boreholes. Models for practical engineering designs are often oversimplified in dealing with the complicated geometry inside the boreholes. A one-dimensional model [1] has been recommended, conceiving the legs of the U-tubes as a single "equivalent pipe" inside the borehole, which leads to a simple expression

$$R_b = \frac{1}{2\pi k_b} \ln\left(\frac{r_b}{\sqrt{N} r_p}\right) + R_p \tag{1}$$

Another effort to describe the borehole resistance has used the concept of the shape factor of conduction and resulted in an expression

$$R_b = \left[k_b \beta_0 \left(\frac{r_b}{r_p} \right)^{\beta_1} \right]^{-1} \tag{2}$$

where parameters β_0 and β_1 were obtained by means of curve fitting of effective borehole resistance determined in laboratory measurements [8]. In this approach only a limited number of influencing factors were considered, and all the pipes were assumed to be of identical temperature as a precondition.

By a different approach Hellstrom [9] has derived two-dimensional analytical solutions of the borehole thermal resistances in the cross-section perpendicular to the borehole with arbitrary numbers of pipes, which are superior to empirical expressions. Also on assumptions of identical temperatures and heat fluxes of all the pipes in it the borehole resistance has been worked out for symmetrically disposed double U-tubes as

$$R_b = \frac{1}{2\pi k_b} \left[\ln\left(\frac{r_b}{r_p} \right) - \frac{3}{4} + \left(\frac{D}{r_b} \right)^2 - \frac{1}{4} \ln\left(1 - \frac{D^8}{r_b^8} \right) - \frac{1}{2} \ln\left(\frac{\sqrt{2}D}{r_p} \right) - \frac{1}{4} \ln\left(\frac{2D}{r_p} \right) \right] + \frac{R_p}{4} \tag{3}$$

Exchanging heat with the surrounding ground, the fluid circulating through different legs of the U-tubes is, in fact, of varying temperatures. As a result, thermal interference, or thermal "short-circuiting", among U-tube legs is inevitable, which degrades the effective heat transfer in the GHEs. With the assumption of identical temperature of all the pipes, it is impossible for all the models mentioned above to reveal impact of this thermal interference on GHE performances.

On the other hand, Mei and Baxter [10] considered the two-dimensional model of the radial and longitudinal heat transfer, which was solved with a finite difference scheme. Recently, Yavuzturk et al. [7] employed the two-dimensional finite element method to analyze the heat conduction in the plane perpendicular to the borehole for short time step responses. Requiring numerical solutions, these models are of limited practical value for use by designers of GCHP systems although they may result in more exact solutions for research and parametric analysis of GHEs.

Taking into account the fluid temperature variation along the borehole depth and its axial convection, the authors have developed a quasi-three-dimensional model to determine analytically the thermal resistance inside boreholes with a single U-tube under arbitrary disposal [11]. The new model reveals the thermal interference between the U-tube pipes, and formulates the borehole heat transfer process on a solid analytical basis. This paper focuses further on discussing heat transfer inside a borehole with double U-tubes. Analytical expressions of the thermal resistance of the double U-tube boreholes are to be derived, and then, performance can be compared between single and double U-tube boreholes.

3. Formulation of heat flow balance

As an extension of the work of Eskilson [12] and Hellstrom [9], following analysis focuses on heat transfer inside the borehole, which serves as a part of the entire thermal process in the GHEs. To keep the problem analytically manageable some simplifications are assumed. They are

(1) The heat capacity of the materials inside the borehole is neglected.
(2) The heat conduction in the axial direction is negligible, and only the conductive heat flow among the borehole wall and the pipes in the transverse cross-section is counted.
(3) The borehole wall temperature, T_b, is constant along its depth, but may vary with time.
(4) The ground outside the borehole and grout in it are homogeneous, and all the thermal properties involved are independent of temperature.

Number the pipes in the borehole clockwise as shown in Fig. 2. If the temperature on the borehole wall, T_b, is taken as the reference of the temperature excess, the temperature excess distribution inside the borehole and the fluid temperature in the pipes may be expressed as the sum of four separate temperature excesses caused by the heat fluxes per unit length, q_1, q_2, q_3 and q_4 from the four legs of the U-tubes. Thus, the following expressions may be obtained

$$\begin{aligned} T_{f1} - T_b &= R_{11}q_1 + R_{12}q_2 + R_{13}q_3 + R_{14}q_4 \\ T_{f2} - T_b &= R_{21}q_1 + R_{22}q_2 + R_{23}q_3 + R_{24}q_4 \\ T_{f3} - T_b &= R_{31}q_1 + R_{32}q_2 + R_{33}q_3 + R_{34}q_4 \\ T_{f4} - T_b &= R_{41}q_1 + R_{42}q_2 + R_{43}q_3 + R_{44}q_4 \end{aligned} \tag{4}$$

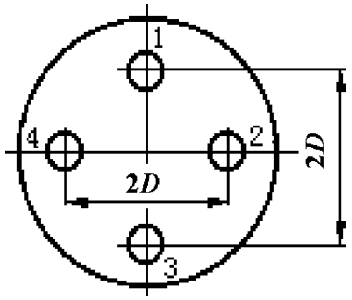

Fig. 2. Cross-section of a double U-tubes borehole.

where R_{ii} $(i = 1, 2, 3, 4)$ is the thermal resistance between the circulating fluid in a certain U-tube leg and the borehole wall, and R_{ij} $(i, j = 1, 2, 3, 4)$ the resistance between two individual pipes. It is most likely that in engineering practice the U-tube legs are disposed in the borehole symmetrically as shown in Fig. 2. In this case one gets $R_{ij} = R_{ji}$, $R_{ii} = R_{jj}$ $(i, j = 1, 2, 3, 4)$ and $R_{14} = R_{12}$ and so on. Hellstrom [9] analyzed the steady-state conduction problem in the borehole cross-section in detail with the line-source and multipole approximations. The line-source assumption has resulted in the following solution

$$\begin{aligned} R_{11} &= \frac{1}{2\pi k_b}\left[\ln\left(\frac{r_b}{r_p}\right) - \frac{k_b - k}{k_b + k}\ln\left(\frac{r_b^2 - D^2}{r_b^2}\right)\right] + R_p \\ R_{12} &= \frac{1}{2\pi k_b}\left[\ln\left(\frac{r_b}{\sqrt{2}D}\right) - \frac{k_b - k}{2(k_b + k)}\ln\left(\frac{r_b^4 + D^4}{r_b^4}\right)\right] \\ R_{13} &= \frac{1}{2\pi k_b}\left[\ln\left(\frac{r_b}{2D}\right) - \frac{k_b - k}{k_b + k}\ln\left(\frac{r_b^2 + D^2}{r_b^2}\right)\right] \end{aligned} \tag{5}$$

where k denotes the thermal conductivity of soil/rock around the borehole, while k_b the conductivity of grouting material, and R_p the heat transfer resistance from the fluid inside the U-tubes to the pipe outer surface.

A linear transformation of Eq. (4) leads to

$$\begin{aligned} q_1 &= \frac{T_{f1} - T_b}{R_1^\Delta} + \frac{T_{f1} - T_{f2}}{R_{12}^\Delta} + \frac{T_{f1} - T_{f3}}{R_{13}^\Delta} + \frac{T_{f1} - T_{f4}}{R_{12}^\Delta} \\ q_2 &= \frac{T_{f2} - T_{f1}}{R_{12}^\Delta} + \frac{T_{f2} - T_b}{R_1^\Delta} + \frac{T_{f2} - T_{f3}}{R_{12}^\Delta} + \frac{T_{f2} - T_{f4}}{R_{13}^\Delta} \\ q_3 &= \frac{T_{f3} - T_{f1}}{R_{13}^\Delta} + \frac{T_{f3} - T_{f2}}{R_{12}^\Delta} + \frac{T_{f3} - T_b}{R_1^\Delta} + \frac{T_{f3} - T_{f4}}{R_{12}^\Delta} \\ q_4 &= \frac{T_{f4} - T_{f1}}{R_{12}^\Delta} + \frac{T_{f4} - T_{f2}}{R_{13}^\Delta} + \frac{T_{f4} - T_{f3}}{R_{12}^\Delta} + \frac{T_{f4} - T_b}{R_1^\Delta} \end{aligned} \tag{6}$$

where

$$R_1^\Delta = R_{11} + R_{13} + 2R_{12}$$

$$R_{12}^\Delta = \frac{R_{11}^2 + R_{13}^2 + 2R_{11}R_{13} - 4R_{12}^2}{R_{12}}$$

$$R_{13}^\Delta = \frac{(R_{11} - R_{13})(R_{11}^2 + R_{13}^2 + 2R_{11}R_{13} - 4R_{12}^2)}{R_{13}^2 + R_{11}R_{13} - 2R_{12}^2}$$

Ignoring the convective transfer of the fluid in the axial direction, the two-dimensional approach of the problem has to assume that the temperatures and heat fluxes of the circulating fluid in the individual pipes are identical. This simplification leads to Eq. (3) for the symmetric double U-tube boreholes. It is impossible for this model to reveal the impact of thermal short-circuiting among the U-tube legs on the performance of the GHE. Our study on the single U-tube borehole has shown that this simplification may result in considerable distortion of the borehole resistance [13].

So, the fluid temperature variation along the channels ought be taken into consideration. In order to keep the model concise and analytically manageable, the conductive heat flow in the grout and ground in the axial direction, however, is

still neglected. We refer to this model as quasi-three-dimensional. In this model the convective heat flow along the fluid channels is balanced by the conductive heat flows among the fluid channels and borehole wall. According to Eq. (6) the heat equilibrium of the fluid in individual pipes can be formulated as

$$\begin{aligned}
\pm Mc\frac{\mathrm{d}T_{\mathrm{f}1}(z)}{\mathrm{d}z} &= \frac{T_{\mathrm{f}1}(z)-T_{\mathrm{b}}}{R_1^{\Delta}}+\frac{T_{\mathrm{f}1}(z)-T_{\mathrm{f}2}(z)}{R_{12}^{\Delta}}+\frac{T_{\mathrm{f}1}(z)-T_{\mathrm{f}3}(z)}{R_{13}^{\Delta}}+\frac{T_{\mathrm{f}1}(z)-T_{\mathrm{f}4}(z)}{R_{12}^{\Delta}}\\
\pm Mc\frac{\mathrm{d}T_{\mathrm{f}2}(z)}{\mathrm{d}z} &= \frac{T_{\mathrm{f}2}(z)-T_{\mathrm{f}1}(z)}{R_{12}^{\Delta}}+\frac{T_{\mathrm{f}2}(z)-T_{\mathrm{b}}}{R_1^{\Delta}}+\frac{T_{\mathrm{f}2}(z)-T_{\mathrm{f}3}(z)}{R_{12}^{\Delta}}+\frac{T_{\mathrm{f}2}(z)-T_{\mathrm{f}4}(z)}{R_{13}^{\Delta}}\\
\pm Mc\frac{\mathrm{d}T_{\mathrm{f}3}(z)}{\mathrm{d}z} &= \frac{T_{\mathrm{f}3}(z)-T_{\mathrm{f}1}(z)}{R_{13}^{\Delta}}+\frac{T_{\mathrm{f}3}(z)-T_{\mathrm{f}2}(z)}{R_{12}^{\Delta}}+\frac{T_{\mathrm{f}3}(z)-T_{\mathrm{b}}}{R_1^{\Delta}}+\frac{T_{\mathrm{f}3}(z)-T_{\mathrm{f}4}(z)}{R_{12}^{\Delta}}\\
\pm Mc\frac{\mathrm{d}T_{\mathrm{f}4}(z)}{\mathrm{d}z} &= \frac{T_{\mathrm{f}4}(z)-T_{\mathrm{f}1}(z)}{R_{12}^{\Delta}}+\frac{T_{\mathrm{f}4}(z)-T_{\mathrm{f}2}(z)}{R_{13}^{\Delta}}+\frac{T_{\mathrm{f}4}(z)-T_{\mathrm{f}3}(z)}{R_{12}^{\Delta}}+\frac{T_{\mathrm{f}4}(z)-T_{\mathrm{b}}}{R_1^{\Delta}}
\end{aligned} \tag{7}$$

Here the sign ± on the left side of the equations depends on the condition whether the fluid flows in the same direction as the z-coordinate, which is designated to be downward. When the fluid moves downwards along the channel the sign is positive, and vice versa. Different flow circuit arrangements will lead to different flow directions in the channels. This formulation indicates that the fluid temperature profiles along the channels satisfy a set of coupled linear differential equations. Combined with certain connecting conditions from the flow circuit arrangement, the energy equilibrium equation can be solved by means of Laplace transforms. Then, the temperature distributions of circulating fluid along the channels can be analytically worked out, and the thermal resistance inside the borehole can be determined more adequately.

In following discussions some dimensionless variables are defined to make expressions more concise and generalized. They are

$$\Theta_1=\frac{T_{\mathrm{f}1}(z)-T_{\mathrm{b}}}{T_{\mathrm{f}}'-T_{\mathrm{b}}},\quad \Theta_2=\frac{T_{\mathrm{f}2}(z)-T_{\mathrm{b}}}{T_{\mathrm{f}}'-T_{\mathrm{b}}},\quad \Theta_3=\frac{T_{\mathrm{f}3}(z)-T_{\mathrm{b}}}{T_{\mathrm{f}}'-T_{\mathrm{b}}},\quad \Theta_4=\frac{T_{\mathrm{f}4}(z)-T_{\mathrm{b}}}{T_{\mathrm{f}}'-T_{\mathrm{b}}}$$

$$R_1^{*}=\frac{McR_1^{\Delta}}{H},\quad R_{12}^{*}=\frac{McR_{12}^{\Delta}}{H},\quad R_{13}^{*}=\frac{McR_{13}^{\Delta}}{H}\quad\text{and}\quad Z=\frac{z}{H}$$

4. Fluid temperature profiles along the borehole depth

The fluid temperature profiles in the flow channels, and, then, the borehole resistance are affected by borehole configuration. As mentioned above, there are single U-tube and double U-tube boreholes. The latter can be arranged in series or parallel flow circuits, and each of them includes a few connecting patterns. All these options have to be analyzed separately.

4.1. Single U-tube ground heat exchanger

The fluid temperature profiles in the single U-tube borehole with arbitrary leg disposal were presented in our previous paper [11]. The solution is introduced here briefly for comparison with those of the double U-tube boreholes. In this case there are only two pipes in the borehole, i.e. those numbered 1 and 3, or 2 and 4, in Fig. 2. Designate the fluid temperature of downward and upward flows as T_{d} and T_{u}, and the dimensionless energy equilibrium equation can be expressed a

$$\left.\begin{aligned}
-\frac{\mathrm{d}\Theta_{\mathrm{d}}}{\mathrm{d}Z} &= \frac{\Theta_{\mathrm{d}}}{S_1}+\frac{\Theta_{\mathrm{d}}-\Theta_{\mathrm{u}}}{S_{12}}\\
\frac{\mathrm{d}\Theta_{\mathrm{u}}}{\mathrm{d}Z} &= \frac{\Theta_{\mathrm{u}}-\Theta_{\mathrm{d}}}{S_{12}}+\frac{\Theta_{\mathrm{u}}}{S_1}
\end{aligned}\right\}\quad 0\leqslant Z\leqslant 1 \tag{8}$$

where

$$\Theta_{\mathrm{d}}=\frac{T_{\mathrm{d}}(z)-T_{\mathrm{b}}}{T_{\mathrm{f}}'-T_{\mathrm{b}}},\qquad \Theta_{\mathrm{u}}=\frac{T_{\mathrm{u}}(z)-T_{\mathrm{b}}}{T_{\mathrm{f}}'-T_{\mathrm{b}}}$$

and the two-dimensionless thermal resistances, i.e. S_1 and S_{12} can be worked out as

$$S_1 = \frac{Mc}{H}(R_{11} + R_{13})$$
$$S_{12} = \frac{Mc}{H} \cdot \frac{R_{11}^2 - R_{13}^2}{R_{13}} \tag{9}$$

With the coupling conditions, $\Theta_d(1) = \Theta_u(1)$ and $\Theta_d(0) = 1$, the solution of Eq. (8) can be written as

$$\Theta_d(Z) = \mathrm{ch}(\beta Z) - \frac{1}{\beta S_{12}}\left[\left(\frac{S_{12}}{S_1} + 1\right) - \frac{\beta S_1 \cdot \mathrm{ch}(\beta) - 1}{\beta S_1 \cdot \mathrm{ch}(\beta) + 1}\right]\mathrm{sh}(\beta Z)$$
$$\Theta_u(Z) = \frac{\beta S_1 \cdot \mathrm{ch}(\beta) - 1}{\beta S_1 \cdot \mathrm{ch}(\beta) + 1}\mathrm{ch}(\beta Z) - \frac{1}{\beta S_{12}}\left[1 - \left(\frac{S_{12}}{S_1} + 1\right)\frac{\beta S_1 \cdot \mathrm{ch}(\beta) - 1}{\beta S_1 \cdot \mathrm{ch}(\beta) + 1}\right]\mathrm{sh}(\beta Z) \tag{10}$$

where

$$\beta = \sqrt{\frac{1}{S_1^2} + \frac{2}{S_1 S_{12}}}$$

In consequence, the outlet fluid temperature for single U-tube GHE is

$$\Theta'' = \frac{\beta S_1 \cdot \mathrm{ch}(\beta) - 1}{\beta S_1 \cdot \mathrm{ch}(\beta) + 1} \tag{11}$$

4.2. Double U-tubes in parallel circuit

For the two U-tubes in the borehole connected in parallel circuit, different combinations of circuit arrangement come down to two options that make difference to its heat transfer. They may be represented by notations of (1-3, 2-4) and (1-2, 3-4). Here 1-3 denotes that the fluid flows through pipes 1 and 3 as indicated in Fig. 2, and also through pipes 2 and 4 in parallel. Ignoring difference in mass flow rates in the two U-tubes, and assuming symmetric disposal of the pipes, the temperature profiles of the fluid flowing in the same direction may be regarded as identical. Applying these conditions to Eq. (7), studies show that the energy equilibrium equations for both (1-3, 2-4) and (1-2, 3-4) parallel configurations take the same form as Eq. (8) with the only difference in the expression of the dimensionless thermal resistance S_1 and S_2. Thus, the solutions for the double U-tubes in parallel circuit must have the same form as Eq. (10).

4.2.1. (1-3, 2-4) configuration in parallel

In this case we have $T_{f1}(z) = T_{f2}(z) = T_d(z)$ and $T_{f3}(z) = T_{f4}(z) = T_u(z)$ for the symmetric configuration. Then, (7) reduces to the following dimensionless expression

$$\left.\begin{aligned} -\frac{d\Theta_d}{dZ} &= \frac{\Theta_d}{R_1^*} + \frac{\Theta_d - \Theta_u}{\dfrac{R_{12}^* R_{13}^*}{R_{12}^* + R_{13}^*}} \\ \frac{d\Theta_u}{dZ} &= \frac{\Theta_u - \Theta_d}{\dfrac{R_{12}^* R_{13}^*}{R_{12}^* + R_{13}^*}} + \frac{\Theta_u}{R_1^*} \end{aligned}\right\} \quad 0 \leqslant Z \leqslant 1 \tag{12}$$

with coupling conditions $\Theta_d(1) = \Theta_u(1)$ and $\Theta_d(0) = 1$.

Comparing Eq. (12) with Eq. (8), one comes to the conclusion that Eq. (10) represents also the temperature profiles of the (1-3, 2-4) parallel configuration as long as the dimensionless variables S_1 and S_{12} in Eq. (10) are defined otherwise as follows:

$$S_1 = R_1^*$$
$$S_{12} = \frac{R_{12}^* R_{13}^*}{R_{12}^* + R_{13}^*} \tag{13}$$

The borehole with double U-tubes in (1-2, 4-3) parallel configuration is of the same nature as the one in this (1-3, 2-4) configuration.

4.2.2. (1-2, 3-4) configuration in parallel

Similarly, we have $T_{f1}(z) = T_{f3}(z) = T_d(z)$ and $T_{f2}(z) = T_{f4}(z) = T_u(z)$ in this case. Then, Eq. (7) is reduced to the following expression

$$\left.\begin{aligned} -\frac{d\Theta_d}{dZ} &= \frac{\Theta_d}{R_1^*} + 2\frac{\Theta_d - \Theta_u}{R_{12}^*} \\ \frac{d\Theta_u}{dZ} &= 2\frac{\Theta_u - \Theta_d}{R_{12}^*} + \frac{\Theta_u}{R_1^*} \end{aligned}\right\} \quad 0 \leqslant Z \leqslant 1 \tag{14}$$

with the same coupling conditions $\Theta_d(1) = \Theta_u(1)$ and $\Theta_d(0) = 1$.

The temperature profiles of the (1-2, 3-4) parallel configuration take the same expression as Eq. (10) while the dimensionless variables S_1 and S_{12} are defined otherwise as follows:

$$\begin{aligned} S_1 &= R_1^* \\ S_{12} &= \frac{R_{12}^*}{2} \end{aligned} \tag{15}$$

4.3. Double U-tubes in series circuit

When the fluid circulates through the four legs of the double U-tubes in a series circuit, there are quite a few possible layouts. Only three of them, however, bear different impact on the performance of GHE on the assumption of symmetrical disposal of the pipes. The three representative layouts in series are marked as 1-3-2-4, 1-2-3-4 and 1-2-4-3, where the sequence indicates flow succession of the pipes as shown in Fig. 2.

4.3.1. 1-3-2-4 configuration in series

In this case the energy equilibrium equation can be normalized as

$$\left.\begin{aligned} -\frac{d\Theta_1(Z)}{dZ} &= \frac{\Theta_1(Z)}{R_1^*} + \frac{\Theta_1(Z) - \Theta_2(Z)}{R_{12}^*} + \frac{\Theta_1(Z) - \Theta_3(Z)}{R_{13}^*} + \frac{\Theta_1(Z) - \Theta_4(Z)}{R_{12}^*} \\ -\frac{d\Theta_2(Z)}{dZ} &= \frac{\Theta_2(Z) - \Theta_1(Z)}{R_{12}^*} + \frac{\Theta_2(Z)}{R_1^*} + \frac{\Theta_2(Z) - \Theta_3(Z)}{R_{12}^*} + \frac{\Theta_2(Z) - \Theta_4(Z)}{R_{13}^*} \\ \frac{d\Theta_3(Z)}{dZ} &= \frac{\Theta_3(Z) - \Theta_1(Z)}{R_{13}^*} + \frac{\Theta_3(Z) - \Theta_2(Z)}{R_{12}^*} + \frac{\Theta_3(Z)}{R_1^*} + \frac{\Theta_3(Z) - \Theta_4(Z)}{R_{12}^*} \\ \frac{d\Theta_4(Z)}{dZ} &= \frac{\Theta_4(Z) - \Theta_1(Z)}{R_{12}^*} + \frac{\Theta_4(Z) - \Theta_2(Z)}{R_{13}^*} + \frac{\Theta_4(Z) - \Theta_3(Z)}{R_{12}^*} + \frac{\Theta_4(Z)}{R_1^*} \end{aligned}\right\} \quad 0 \leqslant Z \leqslant 1 \tag{16}$$

with its dimensionless coupling conditions $\Theta_1(0) = 1$, $\Theta_1(1) = \Theta_3(1)$, $\Theta_3(0) = \Theta_2(0)$ and $\Theta_2(1) = \Theta_4(1)$.

Eq. (16) represents a set of four linear differential equations, which can be solved with Laplace transformation in a straightforward way despite intricacy and tediousness of its derivation, which can be found elsewhere [14]. The temperature profiles in individual pipes along the borehole depth can be expressed in the following form

$$\begin{aligned} \Theta_1(Z) &= E_{11}(Z)\Theta_1(0) + E_{12}(Z)\Theta_2(0) + E_{13}(Z)\Theta_3(0) + E_{14}(Z)\Theta_4(0) \\ \Theta_2(Z) &= E_{12}(Z)\Theta_1(0) + E_{11}(Z)\Theta_2(0) + E_{14}(Z)\Theta_3(0) + E_{13}(Z)\Theta_4(0) \\ \Theta_3(Z) &= -E_{13}(Z)\Theta_1(0) - E_{14}(Z)\Theta_2(0) + E_{33}(Z)\Theta_3(0) + E_{34}(Z)\Theta_4(0) \\ \Theta_4(Z) &= -E_{14}(Z)\Theta_1(0) - E_{13}(Z)\Theta_2(0) + E_{34}(Z)\Theta_3(0) + E_{33}(Z)\Theta_4(0) \end{aligned} \tag{17}$$

where $E_{11}(Z)$, $E_{12}(Z)$, $E_{13}(Z)$, $E_{14}(Z)$, $E_{33}(Z)$ and $E_{34}(Z)$ may be referred to as distribution functions. The detailed expressions of these functions are listed in Appendix A. Based on Eq. (17), the outlet fluid temperature in the case of 1-3-2-4 series configuration can be figured out as

$$\Theta''_{1\text{-}3\text{-}2\text{-}4} = \frac{\dfrac{E_{12}(1) + E_{14}(1)}{E_{13}(1) + E_{11}(1) - E_{34}(1) + E_{14}(1)} - \dfrac{E_{11}(1) + E_{13}(1)}{E_{14}(1) + E_{12}(1) - E_{33}(1) + E_{13}(1)}}{\dfrac{G_{14}(1) - G_{34}(1)}{E_{14}(1) + E_{12}(1) - E_{33}(1) + E_{13}(1)} + \dfrac{E_{33}(1) - E_{13}(1)}{E_{13}(1) + E_{11}(1) - E_{34}(1) + E_{14}(1)}} \tag{18}$$

4.3.2. 1-2-3-4 configuration in series

The energy equilibrium equation in the case of 1-2-3-4 series configuration can be obtained from Eq. (7) as

$$\left.\begin{aligned}
-\frac{\mathrm{d}\Theta_1}{\mathrm{d}Z} &= \frac{\Theta_1}{R_1^*}+\frac{\Theta_1-\Theta_2}{R_{12}^*}+\frac{\Theta_1-\Theta_3}{R_{13}^*}+\frac{\Theta_1-\Theta_4}{R_{12}^*}\\
\frac{\mathrm{d}\Theta_2}{\mathrm{d}Z} &= \frac{\Theta_2-\Theta_1}{R_{12}^*}+\frac{\Theta_2}{R_1^*}+\frac{\Theta_2-\Theta_3}{R_{12}^*}+\frac{\Theta_2-\Theta_4}{R_{13}^*}\\
-\frac{\mathrm{d}\Theta_3}{\mathrm{d}Z} &= \frac{\Theta_3-\Theta_1}{R_{13}^*}+\frac{\Theta_3-\Theta_2}{R_{12}^*}+\frac{\Theta_3}{R_1^*}+\frac{\Theta_3-\Theta_4}{R_{12}^*}\\
\frac{\mathrm{d}\Theta_4}{\mathrm{d}Z} &= \frac{\Theta_4-\Theta_1}{R_{12}^*}+\frac{\Theta_4-\Theta_2}{R_{13}^*}+\frac{\Theta_4-\Theta_3}{R_{12}^*}+\frac{\Theta_4}{R_1^*}
\end{aligned}\right\}\quad 0\leqslant Z\leqslant 1 \tag{19}$$

with coupling conditions $\Theta_1(0)=1$, $\Theta_1(1)=\Theta_2(1)$, $\Theta_2(0)=\Theta_3(0)$ and $\Theta_3(1)=\Theta_4(1)$.

In the same way the temperature profiles of this circuit configuration have been worked out, and their dimensionless expressions can be written as

$$\begin{aligned}
\Theta_1(Z) &= F_{11}(Z)\Theta_1(0)+F_{12}(Z)\Theta_2(0)+F_{13}(Z)\Theta_3(0)+F_{12}(Z)\Theta_4(0)\\
\Theta_2(Z) &= -F_{12}(Z)\Theta_1(0)+F_{22}(Z)\Theta_2(0)-F_{12}(Z)\Theta_3(0)+F_{24}(Z)\Theta_4(0)\\
\Theta_3(Z) &= F_{13}(Z)\Theta_1(0)+F_{12}(Z)\Theta_2(0)+F_{11}(Z)\Theta_3(0)+F_{12}(Z)\Theta_4(0)\\
\Theta_4(Z) &= -F_{12}(Z)\Theta_1(0)+F_{24}(Z)\Theta_2(0)-F_{12}(Z)\Theta_3(0)+F_{22}(Z)\Theta_4(0)
\end{aligned} \tag{20}$$

The distribution functions $F_{11}(Z)$, $F_{12}(Z)$, $F_{13}(Z)$, $F_{22}(Z)$ and $F_{24}(Z)$ can be found in Appendix B. According to Eq. (20) the outlet fluid temperature in the case of 1-2-3-4 series configuration can be obtained as

$$\Theta''_{1\text{-}2\text{-}3\text{-}4}=\frac{\dfrac{F_{13}(1)+F_{12}(1)}{F_{24}(1)-2F_{12}(1)-F_{11}(1)}-\dfrac{F_{11}(1)+F_{12}(1)}{F_{22}(1)-2F_{12}(1)-F_{13}(1)}}{\dfrac{F_{22}(1)-F_{12}(1)}{F_{24}(1)-2F_{12}(1)-F_{11}(1)}-\dfrac{F_{24}(1)-F_{12}(1)}{F_{22}(1)-2F_{12}(1)-F_{13}(1)}} \tag{21}$$

4.3.3. 1-2-4-3 configuration in series

The dimensionless energy equilibrium equation for this configuration can be obtained as

$$\left.\begin{aligned}
-\frac{\mathrm{d}\Theta_1}{\mathrm{d}Z} &= \frac{\Theta_1}{R_1^*}+\frac{\Theta_1-\Theta_2}{R_{12}^*}+\frac{\Theta_1-\Theta_3}{R_{13}^*}+\frac{\Theta_1-\Theta_4}{R_{12}^*}\\
\frac{\mathrm{d}\Theta_2}{\mathrm{d}Z} &= \frac{\Theta_2-\Theta_1}{R_{12}^*}+\frac{\Theta_2}{R_1^*}+\frac{\Theta_2-\Theta_3}{R_{12}^*}+\frac{\Theta_2-\Theta_4}{R_{13}^*}\\
\frac{\mathrm{d}\Theta_3}{\mathrm{d}Z} &= \frac{\Theta_3-\Theta_1}{R_{13}^*}+\frac{\Theta_3-\Theta_2}{R_{12}^*}+\frac{\Theta_3}{R_1^*}+\frac{\Theta_3-\Theta_4}{R_{12}^*}\\
-\frac{\mathrm{d}\Theta_4}{\mathrm{d}Z} &= \frac{\Theta_4-\Theta_1}{R_{12}^*}+\frac{\Theta_4-\Theta_2}{R_{13}^*}+\frac{\Theta_4-\Theta_3}{R_{12}^*}+\frac{\Theta_4}{R_1^*}
\end{aligned}\right\}\quad 0\leqslant Z\leqslant 1 \tag{22}$$

with coupling condition as $\Theta_1(0)=1$, $\Theta_1(1)=\Theta_2(1)$, $\Theta_2(0)=\Theta_4(0)$ and $\Theta_4(1)=\Theta_3(1)$.

The temperature profiles of the 1-2-4-3 configuration have also been obtained. They are

$$\begin{aligned}
\Theta_1(Z) &= G_{11}(Z)\Theta_1(0)+G_{12}(Z)\Theta_2(0)+G_{13}(Z)\Theta_3(0)+G_{14}(Z)\Theta_4(0)\\
\Theta_2(Z) &= -G_{12}(Z)\Theta_1(0)+G_{22}(Z)\Theta_2(0)+G_{23}(Z)\Theta_3(0)-G_{13}(Z)\Theta_4(0)\\
\Theta_3(Z) &= -G_{13}(Z)\Theta_1(0)+G_{23}(Z)\Theta_2(0)+G_{22}(Z)\Theta_3(0)-G_{12}(Z)\Theta_4(0)\\
\Theta_4(Z) &= G_{14}(Z)\Theta_1(0)+G_{13}(Z)\Theta_2(0)+G_{12}(Z)\Theta_3(0)+G_{11}(Z)\Theta_4(0)
\end{aligned} \tag{23}$$

The distribution functions $G_{11}(Z)$, $G_{12}(Z)$, $G_{13}(Z)$, $G_{14}(Z)$, $G_{22}(Z)$ and $G_{23}(Z)$ in this case are presented in Appendix C. Based on Eq. (23), the outlet fluid temperature in the case of 1-2-4-3 series configuration is obtained as

$$\Theta''_{1-2-4-3}=\frac{\dfrac{G_{14}(1)+G_{13}(1)}{G_{23}(1)-G_{12}(1)-G_{13}(1)-G_{11}(1)}+\dfrac{G_{12}(1)+G_{11}(1)}{G_{12}(1)+G_{14}(1)-G_{22}(1)+G_{13}(1)}}{\dfrac{G_{22}(1)-G_{12}(1)}{G_{23}(1)-G_{12}(1)-G_{13}(1)-G_{11}(1)}-\dfrac{G_{13}(1)-G_{23}(1)}{G_{12}(1)+G_{14}(1)-G_{22}(1)+G_{13}(1)}} \tag{24}$$

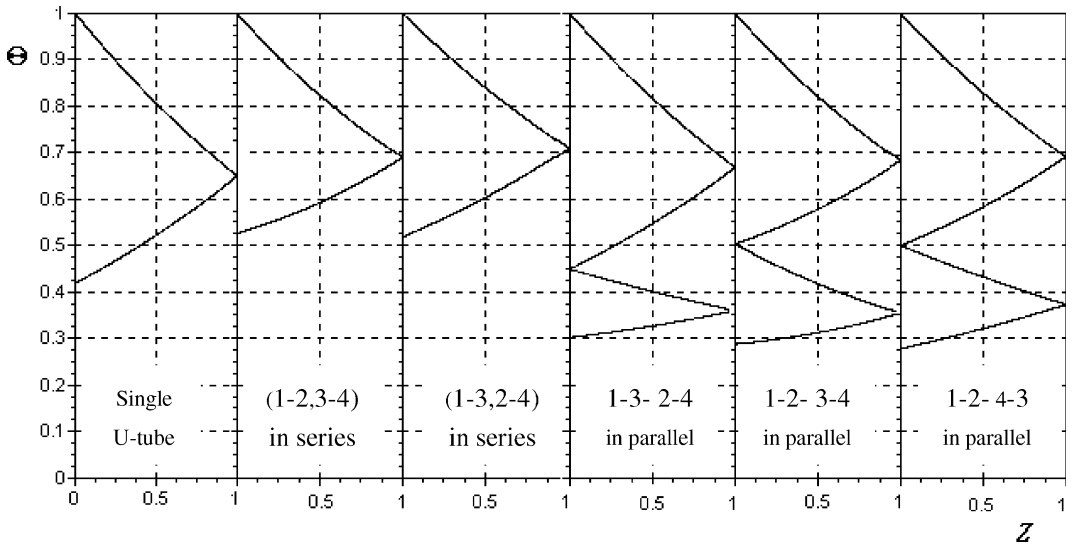

Fig. 3. The temperature profiles along the borehole depth with different borehole configurations.

Table 1
Parameters of the reference borehole

r_b (m)	r_p (m)	H (m)	D (m)	k (W/m K)	k_b (W/m K)	M (kg/s)	c (J/kg K)
0.055	0.016	100	0.030	1.5	1.0	0.2	4187

From the dimensionless formulation of the problem, such as Eq. (12) or (16), it is evident that the dimensionless outlet fluid temperature Θ'' of the double U-tube boreholes is simply a function of three dimensionless resistances R_1^*, R_{12}^* and R_{13}^*.

As a demonstration example, the fluid temperature profiles of the single and double U-tubes in different configurations are calculated and plotted in Fig. 3 for comparison. A typical borehole is chosen as reference and its parameters are listed in Table 1. It can be seen clearly from Fig. 3 that different circulating layouts yield different temperature profiles with different outlet temperatures, which means distinction in their heat transfer performance of the GHEs.

5. Borehole thermal resistance

The effective borehole thermal resistance defines the proportional relationship between the heat flow rate transferred by the borehole and the temperature difference between the circulating fluid and the borehole wall, that is

$$R_b = \frac{T_f - T_b}{q_1} \tag{25}$$

where $T_f = (T_f' - T_f'')/2$ denotes the arithmetic mean of the inlet and outlet fluid temperatures. The borehole thermal resistance takes into account both the geometrical parameters (borehole and pipe sizes and pipe disposal in the borehole) and physical parameters (thermal conductivity of the materials, flow rate and fluid properties). Therefore the concept of effective thermal resistance facilitates heat transfer analysis.

In view of heat balance for the single U-tube and double U-tube in series one also has

$$q_1 H = Mc(T_f' - T_f'') \tag{26}$$

As a result the borehole resistance can be determined according to the analytical solutions of fluid temperature profiles in the borehole presented in previous sections. Combined with the definition of the dimensionless temperature, Eqs. (25) and (26) result in the following expression of the borehole resistance for boreholes with the single U-tube and double U-tubes in series.

Table 2
Borehole thermal resistance R_b of different configurations (K m/W)

H (m)	D (m)	Double U-tube in series configuration			Double U-tubes in parallel configuration		Single U-tube
		1-2-3-4	1-2-4-3	1-3-2-4	(1-2,3-4)	(1-3,2-4)	
40	0.0226	0.1257	0.1255	0.1261	0.1247	0.1245	0.1621
	0.028	0.0999	0.0997	0.1002	0.0990	0.0988	0.1443
	0.034	0.0764	0.0763	0.0767	0.0756	0.0755	0.1274
	0.039	0.0597	0.0596	0.0599	0.0589	0.0587	0.1144
80	0.0226	0.1303	0.1294	0.1320	0.1264	0.1249	0.1641
	0.028	0.1040	0.1033	0.1052	0.1004	0.0997	0.1461
	0.034	0.0802	0.0796	0.0811	0.0768	0.0763	0.1291
	0.039	0.0632	0.0627	0.0640	0.0600	0.0596	0.1160

$$R_b = \frac{H}{2Mc} \cdot \frac{1 + \Theta_f''}{1 - \Theta_f''} \tag{27}$$

In the case of double U-tubes in parallel the fluid mass flow rate in the borehole is doubled, i.e. $2M$, thus the borehole thermal resistance can be expressed as

$$R_b = \frac{H}{4Mc} \cdot \frac{1 + \Theta_f''}{1 - \Theta_f''} \tag{28}$$

The analyses above have shown that even under the condition of axial symmetric disposal of the pipes in the borehole there are quite a few factors that have impact on the borehole resistance, including diameter and depth of the borehole, thermal conductivity and geometric dimensions of the U-tubes, their shank spacing, the thermal conductivities of the backfill and soil/rock around the borehole, fluid flow rate and its thermal properties as well as the flow circuit arrangement. In order to compare the differences in borehole resistances resulted from different circulating layouts calculations were carried out on basis of Eqs. (27) and (28). Again, the parameters were taken from the reference borehole in Table 1 with variations in the borehole depth and U-tube shank spacing. Resulted borehole thermal resistances of different borehole configurations are listed in Table 2.

It can be seen clearly that the borehole thermal resistance decreases noticeably with increase in the U-tube shank spacing. This is easy to understand, for the increase in the shank spacing is favorable to heat conduction between the pipes and the borehole wall while alleviating the thermal interference among U-tube legs. With other parameters unchanged the deeper borehole yields a slightly larger borehole resistance in consequence of its stronger thermal short-circuiting among U-tube legs. Comparisons in Table 2 also demonstrate the ranks of different circulating configurations as the borehole thermal resistance in regards. As expected, the single U-tube boreholes result in considerably higher borehole resistance, up 30% to 90% compared with the corresponding double U-tube boreholes. The double U-tubes in parallel configurations are superior to those in series configurations. Among all the double U-tube configurations the (1-3, 2-4) parallel arrangement yields the lowest borehole resistance although differences among them seem insignificant.

The borehole resistances of the (1-2-4-3) series configuration, (1-3, 2-4) parallel configuration and single U-tube are also plotted in Figs. 4 and 5, calculated on the reference borehole parameters listed in Table 1. Fig. 4 indicates that the borehole thermal resistance decreases with increase in the U-tube shank spacing in all the configurations. Fig. 5 shows that the grout thermal conductivity also bears a significant impact on the borehole thermal resistance, especially when it is relatively small.

6. Conclusions

The effective borehole thermal resistance is of great importance in heat transfer analysis of the GHEs. Previous models for determining the borehole thermal resistance ignore the fluid temperature variation along the channel and fail to take the thermal interference among U-tube pipes into account. Besides, few studies have been available in literature on comparison in heat transfer performance between single and double U-tube boreholes. This paper has presented a

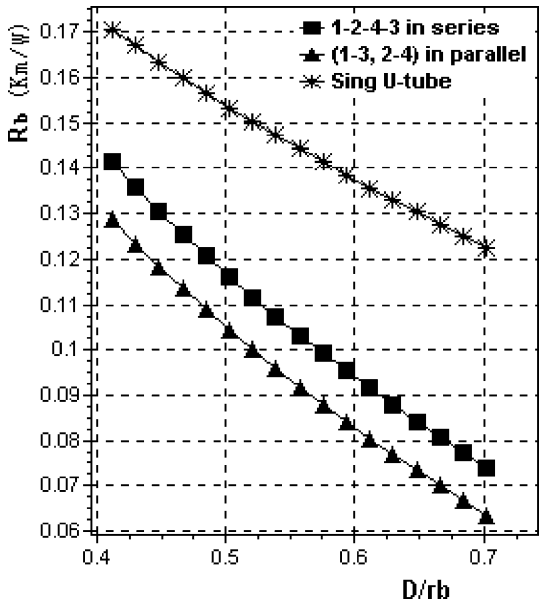

Fig. 4. Relations of borehole thermal resistance to the U-tube shank spacing.

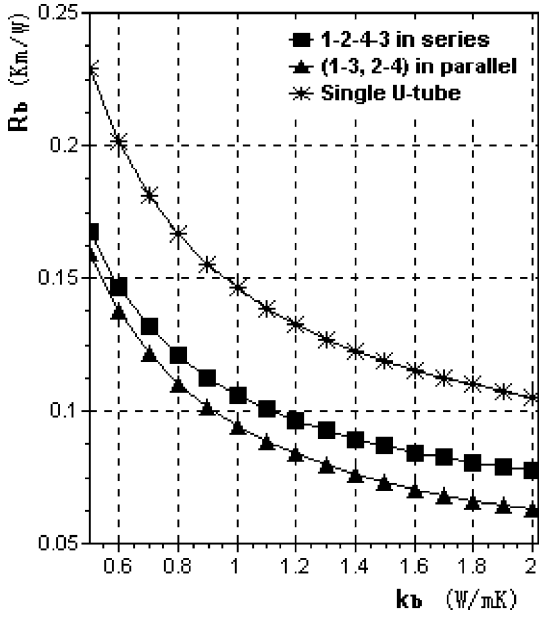

Fig. 5. Relations of borehole thermal resistance to thermal conductivity of backfills.

quasi-three-dimensional model of the borehole heat transfer, and derived analytical solutions of the fluid temperature profiles for single and double U-tube boreholes with all possible circuit layouts. The expressions of the borehole thermal resistance have also been obtained according to the fluid temperature profiles. They take more factors into account than previous models ever did before, including the geometrical parameters (borehole and pipe sizes and pipe disposal in the borehole) and physical parameters (thermal conductivity of the materials, flow rate and fluid properties) as well as the flow circuit configuration. The solutions have provided a reliable tool for GHE sizing and performance simulation and a solid basis for technical and economic assessment of different borehole configurations.

Analyses have shown that the single U-tube boreholes yield considerably higher borehole resistance than their double U-tube counterparts do. The double U-tubes in parallel configuration provide better thermal performance than those in series configuration. Among all the double U-tube configurations the (1-3, 2-4) or (1-2, 4-3) parallel arrangement results in the lowest borehole resistance while differences among them are minor and often negligible in engineering practice.

Calculations on typical GHE boreholes indicate that the U-tube shank spacing and the thermal conductivity of the grout are the prevailing factors in all the configurations considered in determining the borehole thermal resistance. Therefore development of thermally enhanced grouts and improvement on GHE installation techniques are desirable for the purpose of raising overall heat exchange performance.

Finally, discussions in this paper are limited to the thermal resistance inside the boreholes with U-tubes even though the thermal conduction outside the boreholes often plays an even more important role in the GHE heat transfer process. Besides, many factors such as the capital cost of borehole fields and circulating pump energy consumption must also be taken into consideration when merits and weaknesses of different borehole configurations are to be assessed. A detailed economic analysis, however, is beyond the scope of this paper. Nevertheless, the heat transfer models of the GHE boreholes and the expressions derived in this paper may serve as one of the theoretical foundations in performance simulation and economic analysis of GCHP systems.

Appendix A. Distribution functions for 1-3-2-4 configuration in series

$$E_{11}(Z)=\mathrm{ch}(\alpha_e Z)-\frac{A_e}{\alpha_e}\mathrm{sh}(\alpha_e Z)+\frac{2+2A_eR_{13}^*}{R_{12}^*R_{13}^*(\alpha_e^2-\beta_e^2)}[\mathrm{ch}(\alpha_e Z)-\mathrm{ch}(\beta_e Z)]-\frac{A_e\beta_e^2-B_e}{\alpha_e^2-\beta_e^2}\left[\frac{\mathrm{sh}(\alpha_e Z)}{\alpha_e}-\frac{\mathrm{sh}(\beta_e Z)}{\beta_e}\right] \tag{A.1}$$

$$E_{12}(Z)=\frac{\mathrm{sh}(\beta_e Z)}{R_{12}^*\beta_e}-\frac{2A_eR_{13}^*+2}{R_{12}^*R_{13}^*(\alpha_e^2-\beta_e^2)}[\mathrm{ch}(\alpha_e Z)-\mathrm{ch}(\beta_e Z)]+\frac{2R_{12}^*R_{13}^*A_e^2+2A_e(R_{12}^*-R_{13}^*)-2}{R_{12}^*R_{12}^*R_{13}^*(\alpha_e^2-\beta_e^2)}\cdot\left[\frac{\mathrm{sh}(\alpha_e Z)}{\alpha_e}-\frac{\mathrm{sh}(\beta_e Z)}{\beta_e}\right] \tag{A.2}$$

$$E_{13}(Z)=\frac{\mathrm{sh}(\beta_e Z)}{R_{13}^*\beta_e}-\frac{(2A_eR_{13}^*+2)(R_{12}^*+R_{13}^*)}{R_{12}^*R_{12}^*R_{13}^*R_{13}^*(\alpha_e^2-\beta_e^2)}\left[\frac{\mathrm{sh}(\alpha_e Z)}{\alpha_e}-\frac{\mathrm{sh}(\beta_e Z)}{\beta_e}\right] \tag{A.3}$$

$$E_{14}(Z)=\frac{\mathrm{sh}(\beta_e Z)}{R_{12}^*\beta_e}-\frac{(2A_eR_{13}^*+2)(R_{12}^*+R_{13}^*)}{R_{12}^*R_{12}^*R_{13}^*R_{13}^*(\alpha_e^2-\beta_e^2)}\left[\frac{\mathrm{sh}(\alpha_e Z)}{\alpha_e}-\frac{\mathrm{sh}(\beta_e Z)}{\beta_e}\right] \tag{A.4}$$

$$E_{33}(Z)=\mathrm{ch}(\alpha Z)+\frac{A_e}{\alpha_e}\mathrm{sh}(\alpha_e Z)+\frac{2A_eR_{13}^*+2}{R_{12}^*R_{13}^*(\alpha_e^2-\beta_e^2)}[\mathrm{ch}(\alpha_e Z)-\mathrm{ch}(\beta_e Z)]+\frac{A_e\beta_e^2-B_e}{\alpha_e^2-\beta_e^2}\left[\frac{\mathrm{sh}(\alpha_e Z)}{\alpha_e}-\frac{\mathrm{sh}(\beta_e Z)}{\beta_e}\right] \tag{A.5}$$

$$E_{34}(Z)=-\frac{\mathrm{sh}(\beta_e Z)}{R_{12}^*\beta_e}-\frac{2A_eR_{13}^*+2}{R_{12}^*R_{13}^*(\alpha_e^2-\beta_e^2)}[\mathrm{ch}(\alpha_e Z)-\mathrm{ch}(\beta_e Z)]-\frac{2A_e^2R_{12}^*R_{13}^*+2A_e(R_{12}^*-R_{13}^*)-2}{R_{12}^*R_{12}^*R_{13}^*(\alpha_e^2-\beta_e^2)}\left[\frac{\mathrm{sh}(\alpha_e Z)}{\alpha_e}-\frac{\mathrm{sh}(\beta_e Z)}{\beta_e}\right] \tag{A.6}$$

where

$$A_e=\frac{1}{R_1^*}+\frac{2}{R_{12}^*}+\frac{1}{R_{13}^*},\qquad B_e=A_e^3-\frac{2A_e}{R_{12}^*R_{12}^*}-\frac{2}{R_{13}^*R_{12}^*R_{12}^*}-\frac{A_e}{R_{13}^*R_{13}^*}$$

$$\alpha_e=\sqrt{\frac{1}{R_1^*}\left(\frac{1}{R_{11}^*}+\frac{2}{R_{12}^*}+\frac{2}{R_{13}^*}\right)},\qquad \beta_e=\sqrt{\left(\frac{1}{R_1^*}+\frac{2}{R_{12}^*}+\frac{2}{R_{13}^*}\right)\left(\frac{1}{R_1^*}+\frac{4}{R_{12}^*}\right)}$$

Appendix B. Distribution functions for 1-2-3-4 configuration in series

$$F_{11}(Z)=\frac{1}{R_{13}^*}\cdot\left[-\frac{\beta_f+R_{13}^*(A_f-\alpha_f^2)}{\alpha^2-\beta^2}\mathrm{ch}(\alpha_f Z)+\frac{\alpha_f^2+R_{13}^*\beta_f(A_f-\alpha_f^2)}{\alpha(\alpha^2-\beta^2)}\mathrm{sh}(\alpha_f Z)\right]+e^{-\beta_f Z}+\frac{1}{R_{13}^*}\cdot\frac{\beta_f+R_{13}^*(A_f-\alpha_f^2)}{\alpha_f^2-\beta_f^2}e^{-\beta_f Z} \tag{B.1}$$

$$F_{12}(Z)=\frac{\mathrm{sh}(\alpha_{\mathrm{f}}Z)}{R^*_{12}\alpha_{\mathrm{f}}} \tag{B.2}$$

$$F_{13}(Z)=\frac{1}{R^*_{13}}\cdot\left[-\frac{B_{\mathrm{f}}+\beta_{\mathrm{f}}}{\alpha_{\mathrm{f}}^2-\beta_{\mathrm{f}}^2}\mathrm{ch}(\alpha_{\mathrm{f}}Z)+\frac{\alpha_{\mathrm{f}}^2+B_{\mathrm{f}}\beta_{\mathrm{f}}}{\alpha(\alpha_{\mathrm{f}}^2-\beta_{\mathrm{f}}^2)}\mathrm{sh}(\alpha_{\mathrm{f}}Z)+\frac{B_{\mathrm{f}}+\beta_{\mathrm{f}}}{\alpha_{\mathrm{f}}^2-\beta_{\mathrm{f}}^2}\mathrm{e}^{-\beta_{\mathrm{f}}Z}\right] \tag{B.3}$$

$$F_{22}(Z)=-\frac{1}{R^*_{13}}\left[\frac{\beta_{\mathrm{f}}+R^*_{13}(A_{\mathrm{f}}-\alpha_{\mathrm{f}}^2)}{\alpha_{\mathrm{f}}^2-\beta_{\mathrm{f}}^2}\mathrm{ch}(\alpha_{\mathrm{f}}Z)+\frac{\alpha_{\mathrm{f}}^2+R^*_{13}\beta_{\mathrm{f}}(A_{\mathrm{f}}-\alpha_{\mathrm{f}}^2)}{\alpha_{\mathrm{f}}(\alpha_{\mathrm{f}}^2-\beta_{\mathrm{f}}^2)}\mathrm{sh}(\alpha_{\mathrm{f}}Z)\right]+\mathrm{e}^{\beta_{\mathrm{f}}Z}+\frac{1}{R^*_{13}}\cdot\frac{\beta_{\mathrm{f}}+R^*_{13}(A_{\mathrm{f}}-\alpha_{\mathrm{f}}^2)}{\alpha_{\mathrm{f}}^2-\beta_{\mathrm{f}}^2}\mathrm{e}^{\beta_{\mathrm{f}}Z} \tag{B.4}$$

$$F_{24}(Z)=-\frac{1}{R^*_{13}}\left[\frac{\beta_{\mathrm{f}}+B_{\mathrm{f}}}{\alpha_{\mathrm{f}}^2-\beta_{\mathrm{f}}^2}\mathrm{ch}(\alpha_{\mathrm{f}}Z)+\frac{\alpha_{\mathrm{f}}^2+B_{\mathrm{f}}\beta_{\mathrm{f}}}{\alpha(\alpha_{\mathrm{f}}^2-\beta_{\mathrm{f}}^2)}\mathrm{sh}(\alpha_{\mathrm{f}}Z)-\frac{\beta_{\mathrm{f}}+B_{\mathrm{f}}}{\alpha_{\mathrm{f}}^2-\beta_{\mathrm{f}}^2}\mathrm{e}^{\beta_{\mathrm{f}}Z}\right] \tag{B.5}$$

where

$$A_{\mathrm{f}}=\left(\frac{1}{R^*_1}+\frac{2}{R^*_{12}}\right)^2+\frac{1}{R^*_1R^*_{13}}+\frac{2}{R^*_{12}R^*_{13}}-\frac{2}{R^*_{12}R^*_{12}},\qquad B_{\mathrm{f}}=\frac{1}{R^*_1}+\frac{2}{R^*_{12}}+\frac{2R^*_{13}}{R^*_{12}R^*_{12}}$$

$$\alpha_{\mathrm{f}}=\sqrt{\left(\frac{1}{R^*_1}+\frac{4}{R^*_{12}}\right)\frac{1}{R^*_1}},\qquad \beta_{\mathrm{f}}=\frac{1}{R^*_1}+\frac{2}{R^*_{12}}+\frac{2}{R^*_{13}}$$

Appendix C. Distribution functions for 1-2-4-3 configuration in series

$$G_{11}(Z)=\mathrm{ch}(\beta_{\mathrm{g}}Z)-\frac{A_{\mathrm{g}}}{\beta_{\mathrm{g}}}\mathrm{sh}(\beta_{\mathrm{g}}Z)-\frac{\left(\frac{2}{R^*_{12}R^*_{13}}+\frac{2A_{\mathrm{g}}}{R^*_{12}}\right)}{(\alpha_{\mathrm{g}}^2-\beta_{\mathrm{g}}^2)}[\mathrm{ch}(\alpha_{\mathrm{g}}Z)-\mathrm{ch}(\beta_{\mathrm{g}}Z)]$$
$$-\frac{A_{\mathrm{g}}\alpha_{\mathrm{g}}^2-A_{\mathrm{g}}^3+\frac{2A_{\mathrm{g}}}{R^*_{12}R^*_{12}}+\frac{2}{R^*_{13}R^*_{12}R^*_{12}}+\frac{A_{\mathrm{g}}}{R^*_{13}R^*_{13}}}{(\alpha_{\mathrm{g}}^2-\beta_{\mathrm{g}}^2)}\left[\frac{\mathrm{sh}(\alpha_{\mathrm{g}}Z)}{\alpha_{\mathrm{g}}}-\frac{\mathrm{sh}(\beta_{\mathrm{g}}Z)}{\beta_{\mathrm{g}}}\right] \tag{C.1}$$

$$G_{12}(Z)=\frac{\mathrm{sh}(\beta_{\mathrm{g}}Z)}{\beta_{\mathrm{g}}R^*_{12}}+\frac{1}{R^*_{12}}\cdot\frac{\alpha_{\mathrm{g}}^2-A_{\mathrm{g}}^2-\frac{2A_{\mathrm{g}}}{R^*_{13}}-\frac{1}{R^*_{13}R^*_{13}}}{(\alpha_{\mathrm{g}}^2-\beta_{\mathrm{g}}^2)}\left[\frac{\mathrm{sh}(\alpha_{\mathrm{g}}Z)}{\alpha_{\mathrm{g}}}-\frac{\mathrm{sh}(\beta_{\mathrm{g}}Z)}{\beta_{\mathrm{g}}}\right] \tag{C.2}$$

$$G_{13}(Z)=\frac{\mathrm{sh}(\beta_{\mathrm{g}}Z)}{\beta_{\mathrm{g}}R^*_{13}}+\frac{1}{R^*_{13}}\cdot\frac{\alpha_{\mathrm{g}}^2-\frac{2A_{\mathrm{g}}R^*_{13}}{R^*_{12}R^*_{12}}-\frac{2}{R^*_{12}R^*_{12}}-A_{\mathrm{g}}^2+\frac{1}{R^*_{13}R^*_{13}}}{(\alpha_{\mathrm{g}}^2-\beta_{\mathrm{g}}^2)}\left[\frac{\mathrm{sh}(\alpha_{\mathrm{g}}Z)}{\alpha_{\mathrm{g}}}-\frac{\mathrm{sh}(\beta_{\mathrm{g}}Z)}{\beta_{\mathrm{g}}}\right] \tag{C.3}$$

$$G_{14}(Z)=\frac{\mathrm{sh}(\beta_{\mathrm{g}}Z)}{\beta_{\mathrm{g}}R^*_{12}}-\frac{\left(\frac{2}{R^*_{13}}+2A_{\mathrm{g}}\right)}{R^*_{12}(\alpha_{\mathrm{g}}^2-\beta_{\mathrm{g}}^2)}[\mathrm{ch}(\alpha_{\mathrm{g}}Z)-\mathrm{ch}(\beta_{\mathrm{g}}Z)]+\frac{1}{R^*_{12}}\cdot\frac{\alpha_{\mathrm{g}}^2+A_{\mathrm{g}}^2+\frac{2A_{\mathrm{g}}}{R^*_{13}}+\frac{1}{R^*_{13}R^*_{13}}}{(\alpha_{\mathrm{g}}^2-\beta_{\mathrm{g}}^2)}\left[\frac{\mathrm{sh}(\alpha_{\mathrm{g}}Z)}{\alpha_{\mathrm{g}}}-\frac{\mathrm{sh}(\beta_{\mathrm{g}}Z)}{\beta_{\mathrm{g}}}\right] \tag{C.4}$$

$$G_{22}(Z)=\mathrm{ch}(\beta_{\mathrm{g}}Z)+\frac{A_{\mathrm{g}}}{\beta_{\mathrm{g}}}\mathrm{sh}(\beta_{\mathrm{g}}Z)-\frac{\left(\frac{2}{R^*_{12}R^*_{13}}+\frac{2A_{\mathrm{g}}}{R^*_{12}}\right)}{(\alpha_{\mathrm{g}}^2-\beta_{\mathrm{g}}^2)}[\mathrm{ch}(\alpha_{\mathrm{g}}Z)-\mathrm{ch}(\beta_{\mathrm{g}}Z)]$$
$$+\frac{A_{\mathrm{g}}\alpha_{\mathrm{g}}^2-A_{\mathrm{g}}^2+\frac{2A_{\mathrm{g}}}{R^*_{12}R^*_{12}}+\frac{A_{\mathrm{g}}}{R^*_{13}R^*_{13}}+\frac{2}{R^*_{13}R^*_{12}R^*_{12}}}{(\alpha_{\mathrm{g}}^2-\beta_{\mathrm{g}}^2)}\left[\frac{\mathrm{sh}(\alpha_{\mathrm{g}}Z)}{\alpha_{\mathrm{g}}}-\frac{\mathrm{sh}(\beta_{\mathrm{g}}Z)}{\beta_{\mathrm{g}}}\right] \tag{C.5}$$

$$G_{23}(Z)=-\frac{\mathrm{sh}(\beta_{\mathrm{g}}Z)}{\beta_{\mathrm{g}}R^*_{12}}-\frac{\left(2A_{\mathrm{g}}+\frac{2}{R^*_{13}}\right)}{R^*_{12}(\alpha_{\mathrm{g}}^2-\beta_{\mathrm{g}}^2)}[\mathrm{ch}(\alpha_{\mathrm{g}}Z)-\mathrm{ch}(\beta_{\mathrm{g}}Z)]-\frac{1}{R^*_{12}}\cdot\frac{\alpha_{\mathrm{g}}^2+A_{\mathrm{g}}^2+\frac{2A_{\mathrm{g}}}{R^*_{13}}+\frac{1}{R^*_{13}R^*_{13}}}{(\alpha_{\mathrm{g}}^2-\beta_{\mathrm{g}}^2)}\left[\frac{\mathrm{sh}(\alpha_{\mathrm{g}}Z)}{\alpha_{\mathrm{g}}}-\frac{\mathrm{sh}(\beta_{\mathrm{g}}Z)}{\beta_{\mathrm{g}}}\right] \tag{C.6}$$

where

$$A_{\mathrm{g}}=\frac{1}{R^*_1}+\frac{2}{R^*_{12}}+\frac{1}{R^*_{13}}$$

$$\alpha_g = \sqrt{A_g^2 - \left(\frac{1}{R_{13}^*}\right)^2 - \frac{2}{R_{12}^* R_{13}^*} - \frac{2A_g}{R_{12}^*}}$$

$$\beta_g = \sqrt{A_g^2 - \left(\frac{1}{R_{13}^*}\right)^2 + \frac{2}{R_{12}^* R_{13}^*} + \frac{2A_g}{R_{12}^*}}$$

References

[1] J.E. Bose, J.D. Parker, F.C. McQuiston, Design/Data Manual for Closed-Loop Ground Coupled Heat Pump Systems, Oklahoma State University for ASHRAE, Stillwater, 1985.

[2] Caneta Research Inc., Commercial/institutional ground source heat pump engineering manual, American Society of Heating, Refrigerating and Air-Conditioning Engineers (ASHRAE), Atlanta, 1995.

[3] L. Rybach, B. Sanner, Ground-source heat pump systems—the European experience, Geo-Heat Center Quarterly Bulletin. Klamath Falls. Oreg. Oregon Institute of Technology, vol. 21(1), 2000, pp. 16–26.

[4] H.S. Carslaw, J.C. Jeager, Conduction of Heat in Solids, second ed., Oxford Press, Oxford, 1959.

[5] H.Y. Zeng, N.R. Diao, Z.H. Fang, A finite line-source model for boreholes in geothermal heat exchangers, Heat Transfer—Asian Res. 31 (7) (2002) 558–567.

[6] Z.H. Fang, N.R. Diao, P. Cui, Discontinuous operation of geothermal heat exchangers, Tsinghua Sci. Technol. 7 (2) (2002) 194–197.

[7] C. Yavuzturk, J.D. Spitler, S.J. Rees, A transient two-dimensional finite volume model for the simulation of vertical U-tube ground heat exchangers, ASHRAE Trans. 105 (2) (1999) 465–474.

[8] N.D. Paul, The effect of grout conductivity on vertical heat exchanger design and performance, Master Thesis, South Dakota State University, 1996.

[9] G. Hellstrom, Ground heat storage, Thermal analysis of duct storage systems. Doctoral Thesis, Department of Mathematical Physics, University of Lund, Lund, Sweden, 1991.

[10] V.C. Mei, V.D. Baxter, Performance of a ground-coupled heat pump with multiple dissimilar U-tube coils in series, ASHRAE Trans. 92 (Part 2) (1986) 22–25.

[11] H.Y. Zeng, Z.H. Fang, A fluid temperature model for vertical U-tube geothermal heat exchangers, J. Shandong Inst. Archit. Engng. 17 (1) (2002) 7–10.

[12] P. Eskilson, Thermal analysis of heat extraction boreholes, Doctoral Thesis, Department of mathematical Physics, University of Lund, Lund, Sweden, 1987.

[13] H.Y. Zeng, N.R. Diao, Z.H. Fang, Efficiency of vertical geothermal heat exchangers in ground source heat pump systems, J. Thermal Sci. 12 (1) (2003) 77–81.

[14] H.Y. Zeng, Z.H. Fang, A heat transfer model for double U-tube geothermal heat exchangers, J. Shandong Inst. Archit. Engng. 18 (1) (2003) 11–17.